X-625-71-92
PREPRINT



# EXPLORER 35 OBSERVATIONS OF SOLAR WIND ELECTRON DENSITY, TEMPERATURE, AND ANISOTROPY

G. P. SERBU

MARCH 1971



GSFC
GODDARD SPACE FLIGHT CENTER
GREENBELT, MARYLAND

# EXPLORER 35 OBSERVATIONS OF SOLAR WIND ELECTRON DENSITY, TEMPERATURE AND ANISOTROPY

by

G. P. Serbu
Laboratory for Planetary Atmospheres
NASA/Goddard Space Flight Center
Greenbelt, Maryland 20771

## ABSTRACT

Measurements of the electron integral spectrum yield electron temperatures in the range from 1 to $5 \times 10^5$ $^oK$, electron densities at an average value of 4.6 $cm^{-3}$, and electron temperature anisotropies in the range from 1 to 1.4. The electron temperature is found to be independent of solar wind speed over the range from 290 to 675 km $sec^{-1}$. Comparison between the simultaneous alignment of the local magnetic field vector and the direction of the anisotropy reveals a high correlation, indicating that under average conditions the electron energy flow in the solar wind is field aligned. Short-duration field aligned increases in anisotropy associated with large geomagnetic disturbances have been measured to values as high as 3.4. The left-hand mode of the Firehose instability was observed in the electron plasma immediately behind an interplanetary shock.

## INTRODUCTION

Quantitative measurements of the solar wind electron component have been obtained with the hemispherical plate electrostatic analyzer on the Vela 4B satellite (Montgomery, et al., 1968), and the two Pioneer spacecraft experiments: 1. The quadrispherical analyzer (Wolfe and McKibbin, 1968) and 2. the Faraday cup plasma sensor (Formisano, 1969). From these measurements a large body of data is available on the solar wind electron temperature, density, temperature anisotropy and energy content.

The electron temperature ($T_e$) is found to be remarkably uniform over long periods, with the variations restricted over the range from $0.7 \times 10^5$ °K to $2 \times 10^5$ °K, the average value being $1.5 \times 10^5$ °K. The average observed solar wind electron to ion temperature ratio is $T_e/T_i = 3$ (Hundhausen, 1969). Whipple and Parker (1969a) also obtained a value of 3 for this ratio from measurements on Explorer 27. Ogilvie and Ness (1969) suggest that the approximate relationship, $T_e \cong 2\ T_i$ is useful in estimating the electron temperature from ion temperature measurements.

The Vela 4B measurements of electron temperature have demonstrated the existance of an electron thermal anisotropy ($K_e$). The magnitude of this anisotropy is in the range $1.1 \leq K_e \leq 1.2$. From the observations it was inferred that the anisotropy is aligned in the direction of the local

magnetic field. On Pioneer 6 Formisano (op. cit.) showed the anisotropy to be field aligned, with the magnitude as high as 1.4, however, occasionally the data indicated that for substantially long periods (~10 hours) the electron temperature was isotropic, viz. $K_e = 1$.

Measurements of the integral spectrum of the solar wind electrons have been made using a Retarding Potential Analyzer (RPA) experiment, flown on the Moon orbiting spacecraft Explorer 35 (Serbu,1969). The RPA results presented here are generally in good agreement with the published data. A well defined increase in magnitude of the temperature anisotropy has been observed in the solar wind plasma. This increase is associated with the passage of a shock front, which subsequently results in a Sudden Commencement (SC) storm on the Earth. This interesting feature of the data is discussed in light of present theory on solar wind instabilities.

RESULTS

The RPA experiment flown on Explorer 35 was designed to measure the integral spectrum of charged particles over the energy range from 0 to 500 eV. The principle of operation of this experiment has been discussed previously and the interested reader is referred to the literature for a more detailed discription of this and similar experiments (Serbu, op. cit.; Whipple and Parker, 1969b; Serbu and Maier, 1970).

The interpretation of electron trap RPA measurements has been extensively treated by Whipple and Parker (1969b) and specifically for the solar wind region by Whipple and Parker (1969a). They show that Langmuir probe theory is applicable to the interpretation of the measurement provided that extraneous currents due to photoemission and secondary electrons are accounted for; and furthermore, provided that the net charge on the spacecraft does not impose a limiting barrier to the species to be sampled. For the solar wind region the average kinetic energy of a thermal electron is of the order of 15 eV; thus the spacecraft potential ($V_\phi$) will be nonlimiting for $V_\phi \geq -15$ volts.

The histogram of Figure 1 shows the percent distribution of values for the spacecraft-to-plasma potential for Explorer 35. The measurement represents the voltage point on the sweep at which the electron current changes from the retarding region to the accelerating region. The distribution is based on 6198 hourly averaged measurements obtained in the solar wind region with the spacecraft in sunlight for the period from January to December, 1968. Serbu (op. cit.) has shown that while traversing the lunar shadow the potential of Explorer 35 shifts rapidly to a more negative value; i.e. -5 volts. Luna-10 also exhibited a similar shift [Gringauz, et al., 1966]. Consequently, measurements obtained in the lunar

shadow have not been included in the histogram of Figure 1.

The measurement indicates that for 87% of the time the potential lies between -3 and -4 volts, the average value being -3.6 volts, therefore, the spacecraft potential is always nonlimiting to electrons. The very stable potential is a consequence of the balance between the net negative charging current of the plasma and the positive charging current due to photoemission and secondary electrons. This observation is indicative of a stable secondary electron yield factor for the spacecraft surface over a one year period.

In the solar wind region, the photoelectrons emitted from the sunlit hemisphere of the spacecraft contribute a current to the measurement which exceeds by more than a factor of 10 the contribution due to the ambient plasma. Consequently, meaningful measurements are made only when the sensor is oriented away from direct sunlight. This restriction precludes a valid measurement of the streaming protons. However, the electrons can be measured by virtue of their large thermal velocity components in the frame of reference moving with the proton bulk velocity. The measured electron plasma current (I) has an expotential dependence of the type

$$I = I_o \exp(- eV/kT_e) \qquad (1)$$

where e is the electronic charge, V is the retarding potential,

k Boltzman's constant, $T_e$ electron temperature, and $I_o$ is the unretarded current, or the current at zero spacecraft-to-plasma potential. For planar geometry the unretarded current ($I_o$) is given by

$$I_o = 1/4\ N_e\ e\ A\ \bar{S} \qquad (2)$$

where $N_e$ is the electron density, e the electronic charge, $\bar{S}$ is the most probable velocity in a Gaussian distribution, and A is the collection area.

The method of least squares was used to fit the data to the above equations, thus the parameters $N_e$ and $T_e$ were determined every 640 seconds. These measurements integrate over all directions in the shaded hemisphere. In a subsequent section the temperature is evaluated as a function of orientation within the shaded hemisphere.

In Figure 2 the hourly averaged values of electron and proton densities as measured on Explorer 35, are plotted for a 12 day period. The retarding potential analyzer measurement of electron density, heavy line, is compared with the Faraday cup measurement of proton density, dotted line. The proton data was furnished by Dr. J.H. Binsack of The Massachusetts Institute of Technology, (Lyons et al., 1967). An abrupt change in the proton thermal velocity from 30 to 75 km $sec^{-1}$ identified the crossing of the bow shock. This crossing is identified on the plot by the vertical dashed line at 15:00 UT, 10 March 1968. At this time the spacecraft crossed into the evening side of the magnetosphere.

For the ten days when the spacecraft was in the solar wind region the two sets of data are in good agreement. For the most part the two curves track each other within 20%. In lieu of an absolute electron density calibration, this comparison shows that the accumulated error in the electron measurement is of the same order as for the protons. In the region near the bow shock and just inside the magnetosphere the electron density is lower by as much as a factor of two. Wolfe and McKibbin, (op. cit.), have shown that within the magnetosheath the electron distribution function shows a steeply rising character. Since the presence of energetic electrons have not been accounted for in the analysis, the magnetosheath density is very likely to be too low.

Figure 3 shows a histogram of the percent occurrence for 6198 measurements of hourly averaged electron density in the solar wind region for the period January to December, 1968. The distribution is skewed with a rapid rise toward the average of 4.6 $cm^{-3}$, and a more gradual slope at higher densities. Hundhausen et al. (1970) critically reviewed the discrepancies among measurements of average proton densities for the years 1962 through 1967. Various investigators having reported densities over the range from 3 to 10 $cm^{-3}$. For 1967 the Vela 3 measurement is $N_p = 7.7$ $cm^{-3}$ with a systematic error of 25%. A similar body of electron density data is not available for comparison.

Thus the value of $N_e$ = 4.6 $cm^{-3}$ for the year 1968 appears to be ~ 40% low when compared to the 1967 proton data, albeit variations of this magnitude might be real from one year to the next.

The histogram for electron temperature over the same time period is shown in Figure 4. Electron temperatures less than 1 x $10^5$ $^oK$ are seldom observed; 90% of the values lie between 1 and 3 x $10^5$ $^oK$, with the average at 1.82 x $10^5$ $^oK$. The average electron thermal energy transport for 1968 is .035 ergs/$cm^2$sec., somewhat larger than the value of .02 ergs/$cm^2$sec. measured in May 1967 by Vela 4B. However, it is only 8% of the energy flow due to the proton bulk flow.

Figure 5 shows a plot of electron temperature, averaged over 25 km $sec^{-1}$ intervals, as a function of proton bulk speed. For the 18 day period from 21 February to 10 March, 1968 the flow speed, as measured by the Faraday cup, exhibited a nearly linear decrease in value from 675 to 325 Km $sec^{-1}$. In addition to the Explorer 35 data points, previous measurements, as referenced in the legend, are shown. Burlaga and Ogilvie (1970) concluded on the basis of the measurements for speeds from 290 to 400 Km $sec^{-1}$ that the electron temperature is nearly independent of flow speed. The Explorer 35 measurements extend these observations to 675 Km $sec^{-1}$ and support their conclusion. These direct measurements are in disagreement with the results of the collisionless 2-fluid solar wind model

(Hollweg, 1970) which predicts that the solar wind velocity at the earth should show a strong correlation with $T_e^{1/2}$.

Explorer 35 is spin-stabilized with the spin axis normal to the ecliptic plane. Therefore, the retarded current (I) will undergo a spin modulation if the velocity distribution is angularly dependent. Such a modulation is expected from a bi-Maxwellian distribution where the electron temperature in one direction differs in magnitude from the temperature perpendicular to it. In order to observe the electron temperature anisotropy the measured retarded current (I) is accumulated over a long time period and then sorted as a function of six separate arrival directions which are evenly distributed over the shaded hemisphere. Figure 6 illustrates the six $30^o$ wide sectors which lie in the ecliptic plane ($X_{sse}$, $Y_{sse}$) and range from $\Phi = 90^o$ to $\Phi = 270^o$. During the observation period defined in Figure 6, a total of 288 measurements of current (I) were obtained as a function of retardation over the voltage interval from +7 to -500 volts. Grouping these measurements according to their orientation in $\Phi$ results in 6 complete current-voltage characteristics, one for each $30^o$ sector. Each characteristic is then analysed using equations 1 and 2.

The electron temperatures for each of the sectors are plotted in Figure 6 as a section of arc, at the radial distance corresponding to the temperature scale shown on the $-Y_{SSE}$ axis. Also shown in Figure 6 are the concurrent

magnetic field observations of Dr. N. F. Ness of Goddard Space Flight Center (Ness et al., 1967), the hourly average values of the field strength F and the two directional angles $\theta$ and $\phi$, are given for the 3 hour period bracketing the electron temperature data. The labelled arrows in the figure correspond to the hourly average values for the magnetic field orientation $\phi$, in the ecliptic plane.

The plot of Figure 6 shows a temperature dependence with orientation in the ecliptic plane. The temperature value is higher in the direction of the local magnetic field vector; i.e. $1.2 \times 10^5$ $^oK$ is observed in the sector centered about $\phi = 105^o \pm 15^o$. The temperature then decreases in value to a minimum of $0.9 \times 10^5$ $^oK$ in the direction perpendicular to the magnetic field, $\phi = 195^o \pm 15^o$. The temperature increases with rotation toward the anti-field direction. The electron temperature anisotropy ($K_e$) is then computed from the ratio of the maximum to minimum values as observed in the anti-solar hemisphere of the spacecraft, viz. $K_e = T_{105^o}/T_{195^o} \simeq T_{\parallel}/T_{\perp} = 1.3$, with the anisotropy directed along the vector $\phi = 105^o \pm 15^o$. Applying the above method the anistropy magnitude, direction, and alignment with the local magnetic field can be observed over extended periods.

Plotted in Figure 7 are the $K_p$ magnetic index, the electron density, and the electron temperature for the 54 hour interval from 06:00UT 19 April to 12:00UT 21 April, 1968. During this period the moon-spacecraft location

projected onto the ecliptic plane at the local hour angle from 0830-1000. The data shown in Figure 7 is therefore representative of the solar wind region, and it was obtained with the spacecraft well removed from the bow shock of the earth. The plot of $K_p$, shown in the top panel of Figure 7 indicates a very quiet magnetic period. The daily sum $K_p$ index for the 19th, 20th, and 21st of April was 5+, 3-, and 8-, respectively. In the lower trace is shown the hourly averaged values of the electron density. During the entire time period only small variations about an average value of 4.8 electrons $cm^{-3}$ are observed. In the middle panel are plotted the electron temperature as measured in each one of the six orientation sectors discussed earlier. The plotting symbols for each sector are shown in the legend. All six sector temperature plots show uniform and steady variations in magnitude about the mean value of $1 \times 10^5$ $^oK$. The electron temperature anisotropy can be observed directly from this plot. The spread among the five curves is a measure of the anisotropy magnitude, and the direction of the anisotropy is taken as that of the sector containing the curve of maximum amplitude. In addition, this plotting format illustrates the temporal variations in anisotropy magnitude and direction. The magnitude of the temperature anisotropy remains almost constant at 1.2 for the entire 54 hour period. However, there are some brief periods such as around 20:00 hours 19 April, and 06:00 hours 20 April when the anisotropy

increases to a value of 1.4.

In Figure 8 are plotted the observed anisotropy direction for the same time period of Figure 7, along with the local magnetic field orientation in the ecliptic plane. The anisotropy data is shown as a shaded block in order to indicate the $\pm 15^{o}$ uncertainty in sector direction, and the $\pm$20 minute averaging interval used in obtaining the data for each sector. The hourly averaged magnetic field direction in the ecliptic plane is plotted as a solid line connecting dark and light data points. The light symbol is used to indicate that the field direction was rotated through $180^{o}$ in order to plot on the scale in $\phi$ from $90^{o}$ to $270^{o}$. Out of the total 54 hours of data plotted in Figure 8, 17 hours correspond primarily to quiet and steady field conditions such as seen around 00:00 UT, 20 April 1968. At these times the agreement between anisotropy direction and field orientation is within the experimental error. For 30 hours out of the total interval the two directions are not more than $30^{o}$ apart. Note for example the 4 hour period around 18:00 UT, 20 April. Essentially no agreement is obtained for the remaining 7 hours. For example shortly after 00:00 UT, 21 April 1968 the field undergoes large changes in direction over a six hour interval and although the anisotropy direction also shows large changes there is essentially no point-to-point agreement. Throughout this entire data interval

the relative strength of the particle to magnetic pressure remained weak; i.e. $\beta_e \leq .75$. Therefore, the lack of agreement in the alignment observed during rapid changes in field direction is more likely associated with the time averaging technique used to obtain the anisotropy, rather then as a result of a plasma instability. The uniform and smooth plot of anisotropy magnitude of Figure 7 is in contrast with the rapid changes in anisotropy direction, see Fig. 8, indicative of the strong coupling of the electrons to the interplanetary magnetic field.

Various effects caused by interplanetary shocks have been discussed by Van Allen and Ness (1967), Ness and Taylor (1968), Sugiura et al. (1968), and Chao and Olbert (1970). Ogilvie, Burlaga, Wilkerson (1968), Burlaga and Ogilvie (1969) have shown that sudden commencement storms are caused by hydromagnetic shocks.

With a fifteen hour interval on the 10th of March 1968 the satellite, Explorer 35, encountered first a magnetohydrodynamic shock and then the Earth's bow shock. Data presented in Figure 9 show that the two shocks exhibit somewhat different electron structures. In Figure 9, the top trace is the $K_p$ hourly value plotted for the period from 18:00 UT, 9 March 1968 until 00:00 UT, 11 March 1968. At 23:40 UT, 9 March, a sudden commencement storm occurred. The storm time is identified on the $K_p$ trace by a solid triangle. For the day previous to the sudden commencement time the magnetic designation was QQ,

with $\Sigma K_p$ = 8-. After the storm, the sum index rose to a value of $\Sigma K_p$ = 22+. In the middle trace are plotted the six sector measurements of electron temperature, the legend identifies the sector in which the temperature data was obtained. In the bottom trace the direction of the electron anisotropy is compared with the direction of the hourly averaged magnetic field vector in the ecliptic. At the time of the sudden commencement, the observed hourly average value for the magnetic field magnitude increased from 6.3$\gamma$ to 10$\gamma$, and the field vector normal to the ecliptic, (i.e. $\theta$ angle) changed from $-4^o$ to $+55^o$. It is difficult to define the average temperature in the presence of the large anisotropy observed subsequent to the shock. A factor of two increase is computed from the data of the remaining five sectors. At the same time the electron density increased from 3 $cm^{-3}$ to 11 $cm^{-3}$. These variations give more than a factor of five increase in the electron pressure behind the shock. Ogilvie et al. (op. cit.) have reported similar values for the increase in the pressure of the proton component across sudden commencement associated shocks. The bottom trace of Figure 9 compares the alignment between the measured anisotropy direction and the direction of the ecliptic component of the interplanetary field. For the entire data period prior to the shock at 23:40 UT the anisotropy was directed along the field vector. Note that at the shock the ecliptic component of the field changed

abruptly from 285° to 265° and the observed anisotropy direction remained field aligned across the shock. As discussed earlier, the anisotropy is observable only in the anti-solar direction. As a consequence the plotting format magnifies the apparent shift in direction whenever the field vector passes through either 90° or 270°. The shaded intervals shown at 0400 UT and 1500 UT indicate that during these times the spacecraft orbital path traversed the lunar shadow. Data for these intervals have been omitted from the plot. Fifteen hours after the shock passage the satellite encountered the Earth's bow shock as it crossed into the evening quadrant of the Magneto-sheath. This crossing was discussed earlier in connection with the data of Figure 2.

Across the bow shock the electron temperature increased from $2.6 \times 10^5$ °K to $4.6 \times 10^5$ °K, and the density remained constant at 5 $cm^{-3}$. The plots of Figure 9 indicate that the electron anisotropy behind the bow shock is greatly enhanced, and that near the bow shock and immediately behind it the electron anisotropy remains field aligned.

Hollweg and Völk (1970) have found a new plasma instability which is driven by anisotropic electrons. This left-hand made of the Firehose instability is shown to have the property of transferring thermal energy from the electrons to the protons, resulting in heating of the solar wind protons. The condition for instability is given by the inequalities

$1-\beta_e A_e < 0$ and $| 1-\beta_e A_e | << 1$. Where $\beta_e$ is the ratio of the electron plasma pressure to the magnetic field pressure ($\beta_e = 4\pi NKT/B^2$), and $A_e$ is the electron anisotropy term ($A_e = 1 - K_e^{-1}$). Normally the product $\beta_e A_e$ is unlikely to exceed unity, thus the criteria might be fulfilled only in small and localized regions of space which contain both density and anisotropy enhancements. The data of Figure 9 suggests that the instability criteria of Hollweg and Völk might be satisfied in connection with interplanetary shocks.

Shown in the last column of Table 1 are the values for the instability criteria ($1 - \beta_e A_e$) as computed from the tabulated hourly magnetic field and plasma data. Data is tabulated for three shocks which were encountered on the 9th and 10th of March, and on the 20th of November, 1968. The data for 15:00 UT, 10 March, was obtained in crossing the bow shock. The other two data sets were obtained at times associated with sudden commencement storms. The condition for instability was satisfied in the plasma immediately behind the interplanetary shock of 23:40 UT, 9 March, viz. at 01:00 UT we calculate $(1 - \beta_e A_e) = - .17$.

Immediately after the interplanetary shock of 09:04 UT, 20 November, the anisotropy was unity. The criteria could not be satisfied even if the magnetic parameters were available. Further note that for the November shock the maximum density peak occurred one hour after the maximum

anisotropy value, whereas on the 9th of March the density and the anisotropy peaked together. After the bow shock crossing, at 16:00 UT the temperature and anisotropy increased, but the concurrent increase in magnetic field maintained the pressure ratio low, i.e. $\beta_e = .60$.

The stringent requirements imposed by simultaneous increases in density, temperature and anisotropy make the observation of the left-hand mode of the Firehose instability very difficult, particularly in view of the large averaging interval required in this measurement of anisotropy. Thus the significants of this instability in heating of the solar wind protons remains to be evaluated by improved observations.

## SUMMARY

Measurements of the integral spectrum of solar wind thermal electrons with a retarding potential analyzer flown on Explorer 35 are found to be in good agreement with previous results. In summary these measurements show that:

a) The spacecraft equilibrium potential in sunlight remained nearly constant at -3.6 volts over a one year period.

b) The average values for electron density and temperature for the year 1968 are: $N_e = 4.6\ cm^{-3}$, $T_e = 1.82 \times 10^5\ ^oK$.

c) The electron temperature was found to be independent of solar wind velocity over the range from 290 to 675 Km $sec^{-1}$.

d) In the quiet solar wind conditions the electron temperature anisotropy ranged in value from 1.0 to 1.4;

the anisotropy was field aligned for better than 85% of the time. Alignment was also observed across interplanetary shocks, in the presence of impulsive directional changes of the local magnetic field.

3) The left-hand mode of the Firehose instability predicted by Hollweg and Völk (1970) was experimentally verified to exist in an extensive region which occurred subsequent to the passage of a interplanetary shock.

ACKNOWLEDGEMENTS

I wish to thank Dr. N. F. Ness for the use of the magnetic field data and Dr. J. H. Binsack for furnishing the solar wind proton data.

## LIST OF FIGURES

Figure 1. The percent distribution of observed spacecraft-to-plasma potential in the solar wind region, for the year 1968.

Figure 2. A 12 day comparison between the measured electron and proton densities, observed simultaneously with different experiments on Explorer 35.

Figure 3. The percent distribution of electron density in the solar wind region for the year 1968.

Figure 4. The percent distribution of electron temperature in the solar wind for the year 1968.

Figure 5. A plot of the electron temperature value as a function of solar wind bulk speed. These observations were made from 21 February to 10 March 1968, the plot includes the previous observations as noted in the legend.

Figure 6. This figure illustrates the six sectors in the $X_{SSE}$, $Y_{SSE}$ plane which evenly divide the darkened hemisphere of the spacecraft. In the figure the sun is at the top, angle $\Phi$ is counterclockwise, and the temperature scale is shown along the $-Y_{SSE}$ axis. The magnetic field amplitude (F) in gammas and the two directional angles $\theta$ and $\Phi$ are tabulated in the legend. The labelled arrows correspond to the sequential magnetic field directions of $\Phi$.

Figure 7. A plot of the electron density and sector temperature (see text) for a 54 hour period during which the planetary magnetic index was less than 1.

Figure 8. A comparison between the direction of the magnetic field component in the ecliptic plane and the observed maximum electron temperature.

Figure 9. Electron temperature and magnetic field observation obtained across a interplanetary shock, and the Earth's bow shock.

## TABLES

Table 1. A tabulation of the magnetic field and electron plasma data associated with the passage of two interplanetary shocks, and one crossing of the Earth's bow shock. The last column tabulates the left-hand Firehose plasma instability term $(1-\beta_e A_e)$.

## REFERENCES


Burlaga, L.F. and K.W. Ogilvie, "Causes of Sudden Commencements and Sudden Impulses", J. Geophys. Res., 74, 2815, 1969.

Burlaga, L.F. and K.W. Ogilvie, "Heating of the Solar Wind", The Astrophysical Journal, Vol. 159, 659, 1970.

Chao, Jih Kwin and Stanislaw Olbert, "Observations of Slow Shocks in Interplanetary Space", J. Geophys. Res., 75, 6394, 1970.

Formisano, V., Interplanetary Plasma Electron - A Preliminary Report of Pioneer 6 Data; J. Geophys. Res., 74, 355, 1969.

Gringauz, K.I., V.V. Bezrukikh, M.Z. Khokhlov, G.I. Zasterker, A.P. Remizov, L.S. Mustov; The Results of Experiments Investigating Plasma in Circumlunar Space With the Aid of Charged Particle Traps on the First Artificial Lunar Satellite. Transl. KOSMICHESKIYE ISS LEDOVANIYA, Vol. 4, No. 6, 851-870, 1966.

Hollweg, Joseph V., "Collisionless Solar Wind 1. Constant Electron Temperature", J. Geophys. Res., 75, 2403, 1970.

Hollweg, J.V. and H.J. Völk, "New Plasma Instabilities in the Solar Wind", J. Geophys. Res., 75, 5297, 1970.

Hundhausen, J.A., "Nonthermal Heating in the Quiet Solar Wind", J. Geophys. Res., 75, 5810, 1969.

Hundhausen, A.J., S.J. Bame, J.R. Asbridge, and S.J. Sydoriak, "Solar Wind Proton Properties: Vela 3 Observations from July 1965 to June 1967", J. Geophys. Res., 75, 4643, 1970.

Lyons, E.F., H.S. Bridge, and J.H. Binsack, "Explorer 35 Plasma Measurements in the Vicinity of the Moon", J. Geophys. Res., 72, 6113, 1967.

Montgomery, Michael D., S.J. Bame, and A.J. Hundhausen, "Solar Wind Electrons: Vela 4 Measurements", J. Geophys.Res., 73, 4999, 1968.

Ness, N.F., K.W. Behannon, C.S. Scearce, and S.C. Cantarano, "Early Results from the Magnetic Field Experiment on Lunar Explorer 35", J. Geophys. Res., 72, 5769, 1967.

Ness, N. F. and H.E. Taylor, "Observations of the Interplanetary Magnetic Field July 4-12, 1966", Annals. of IQSY, 3, 525, 1968.

Ogilvie, K.W., L.F. Burlaga and T.D. Wilkerson, "Plasma Observations of Explorer 34", J. Geophys. Res., 73, 6809, 1968.

Ogilvie, K.W., and N.F. Ness, "Dependence of the Lunar Wake on Solar Wind Plasma Characteristics", J. Geophys. Res., 74, 4123, 1969.

Serbu, G.P., "Explorer 35 Measurements of Low-Engery Plasma in Lunar Orbit", J. Geophys. Res., 74, 372, 1969.

Serbu, G.P., and E.J.R. Maier, "Observations from OGO-5 of the Thermal Ion Density and Temperature Within the Magnetosphere", J. Geophys. Res., 75, 6102, 1970.

Sugiura, M., T.L. Skillman, B.G. Ledley, and J.P. Heppner, "Propagation of the Sudden Commencement of July 8, 1966, to the Magnetotail", J. Geophys. Res., 73, 6699, 1968.

Van Allen, James A., Norman F. Ness, "Observed Particle Effects of an Interplanetary Shock Wave on July 8, 1966", J. Geophys. Res., 72, 935, 1967.

Whipple, Elden C., Lee W. Parker; "Effects of Secondary Electron Emission on Electron Trap Measurements in the Magnetosphere and Solar Wind", J. Geophys. Res., 74, 5763, 1969a.

Whipple, Elden C., Jr., and L. W. Parker, "Theory of an Electron Trap on a Charged Spacecraft", J. Geophys. Res., 74, 2962, 1969b.

Wolfe, J.H., and D.D. McKibbin, Review of Ames Research Center Plasma-Probe Results from Pioneer 6 and 7, Physics of the Magnetosphere, Edited by R.L. Carovillano, J.F. McClay, H.R. Radoski; D. Reiden Publishing Company, Dordrecht-Holland, 1968.

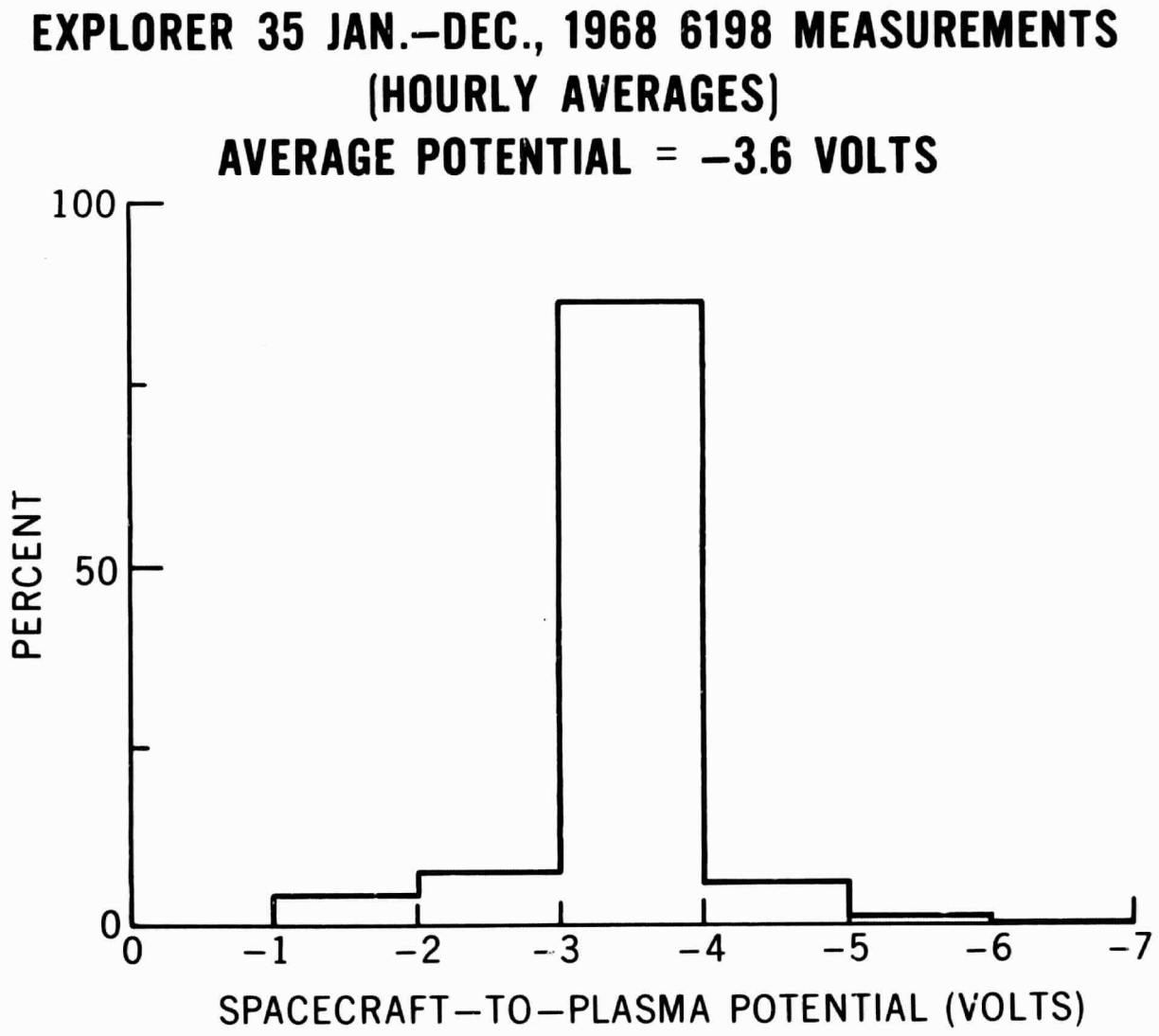
EXPLORER 35 JAN.–DEC., 1968 6198 MEASUREMENTS
(HOURLY AVERAGES)
AVERAGE POTENTIAL = –3.6 VOLTS
100
50
0
PERCENT
0
–1
–2
–3
–4
–5
–6
–7
SPACECRAFT–TO–PLASMA POTENTIAL (VOLTS)

Figure 1

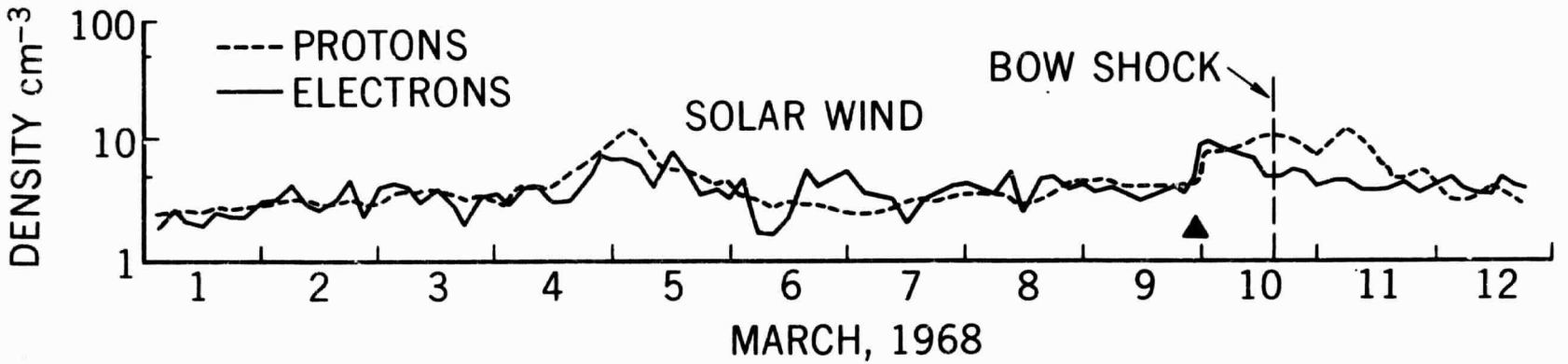
DENSITY cm$^{-3}$
100
10
1
---- PROTONS
—— ELECTRONS
SOLAR WIND
BOW SHOCK
1
2
3
4
5
6
7
8
9
10
11
12
MARCH, 1968

Figure 2

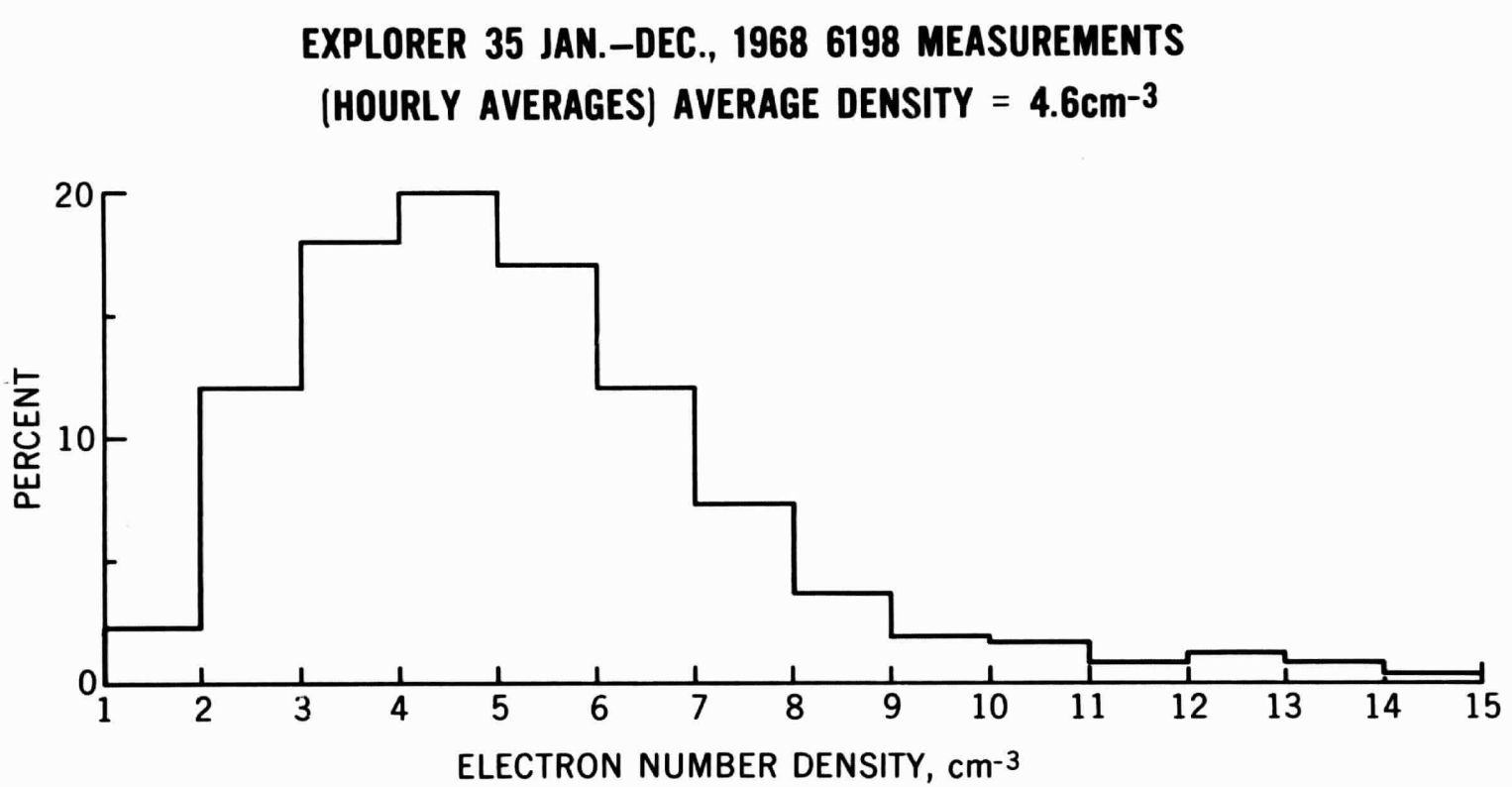
EXPLORER 35 JAN.–DEC., 1968 6198 MEASUREMENTS
(HOURLY AVERAGES) AVERAGE DENSITY = 4.6cm-3
PERCENT
20
10
0
1
2
3
4
5
6
7
8
9
10
11
12
13
14
15
ELECTRON NUMBER DENSITY, cm-3

Figure 3

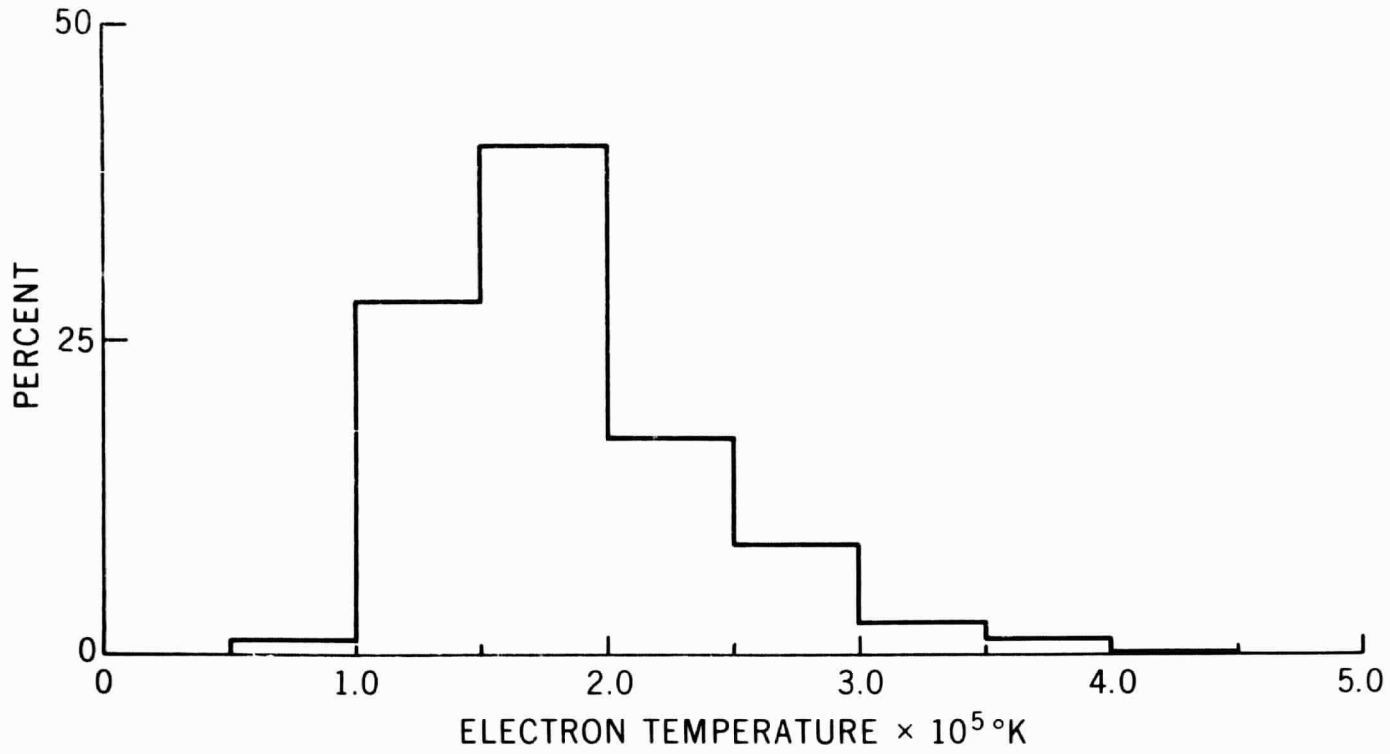
EXPLORER 35 JAN.–DEC., 1968 6198–MEASUREMENTS (HOURLY–AVERAGES)
AVERAGE ELECTRON TEMPERATURE = 1.82 × 10^5 °K
50
25
0
PERCENT
0
1.0
2.0
3.0
4.0
5.0
ELECTRON TEMPERATURE × 10^5 °K

Figure 4

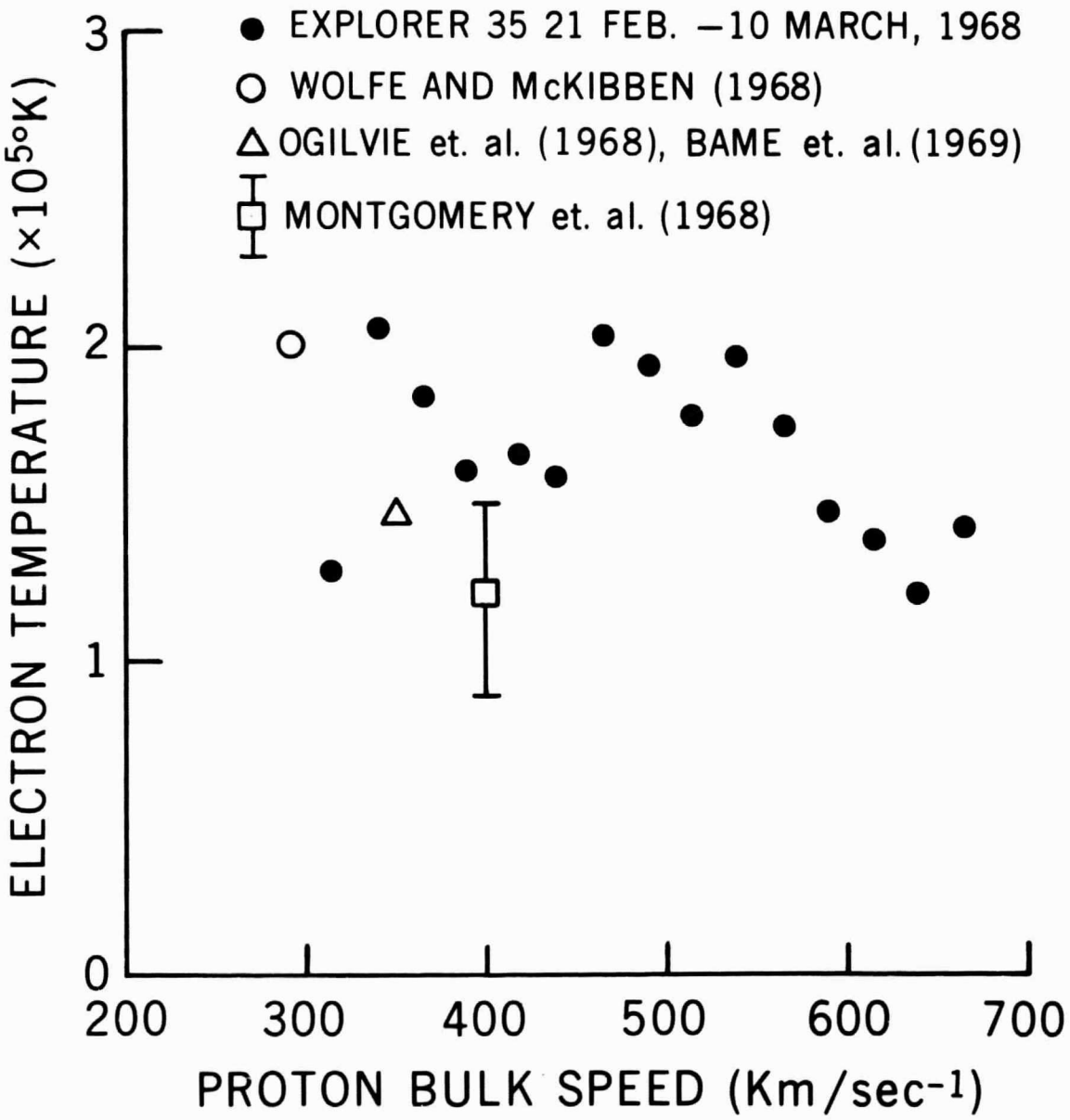
EXPLORER 35 21 FEB. –10 MARCH, 1968
WOLFE AND McKIBBEN (1968)
OGILVIE et. al. (1968), BAME et. al. (1969)
MONTGOMERY et. al. (1968)
ELECTRON TEMPERATURE (×10^5°K)
0
1
2
3
200
300
400
500
600
700
PROTON BULK SPEED (Km/sec-1)

Figure 5

# EXPLORER 35 4/19/68

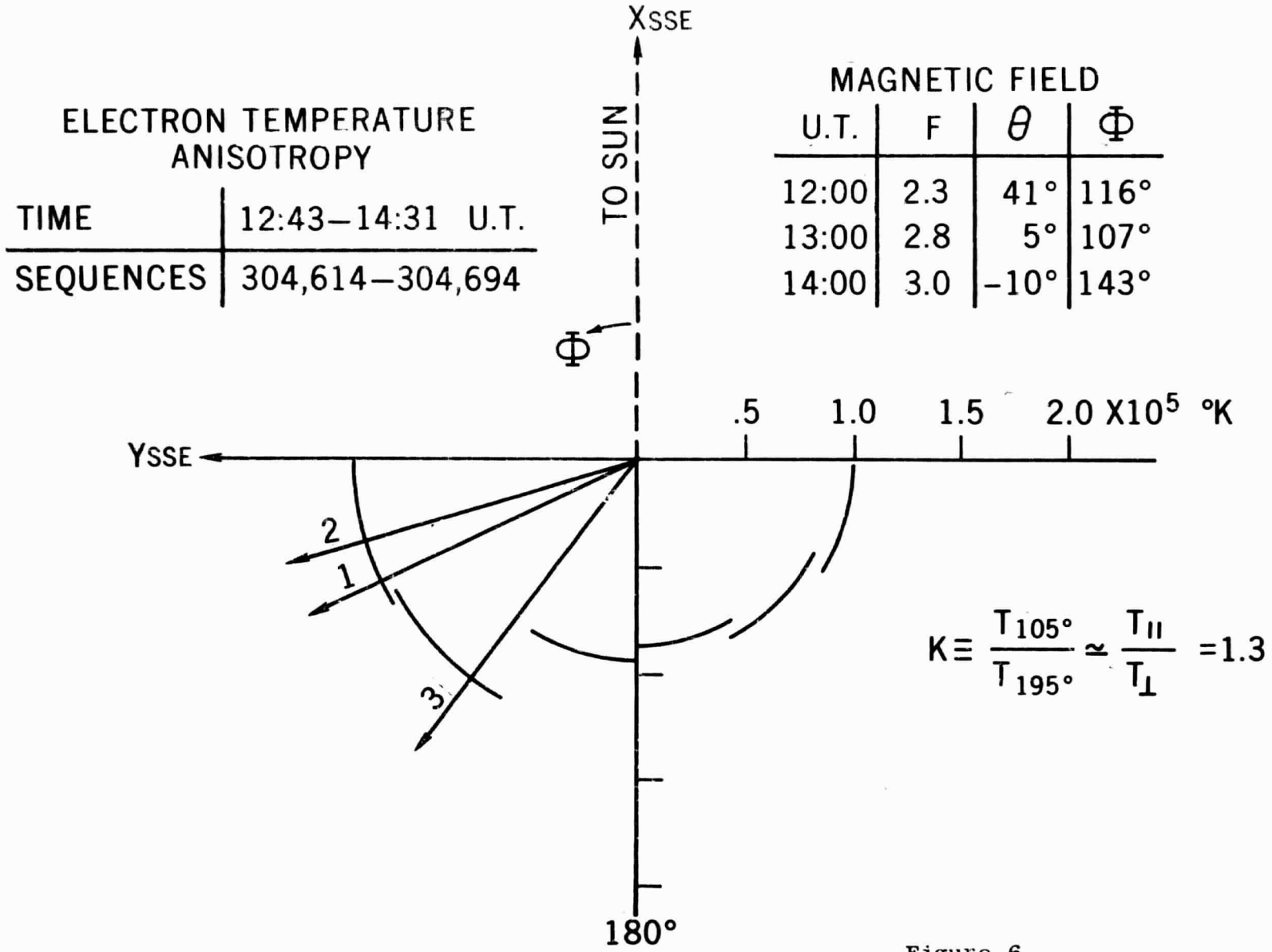


ELECTRON TEMPERATURE ANISOTROPY

| TIME | 12:43–14:31 U.T. |
|---|---|
| SEQUENCES | 304,614–304,694 |

MAGNETIC FIELD

| U.T. | F | θ | Φ |
|---|---|---|---|
| 12:00 | 2.3 | 41° | 116° |
| 13:00 | 2.8 | 5° | 107° |
| 14:00 | 3.0 | −10° | 143° |

Figure 6

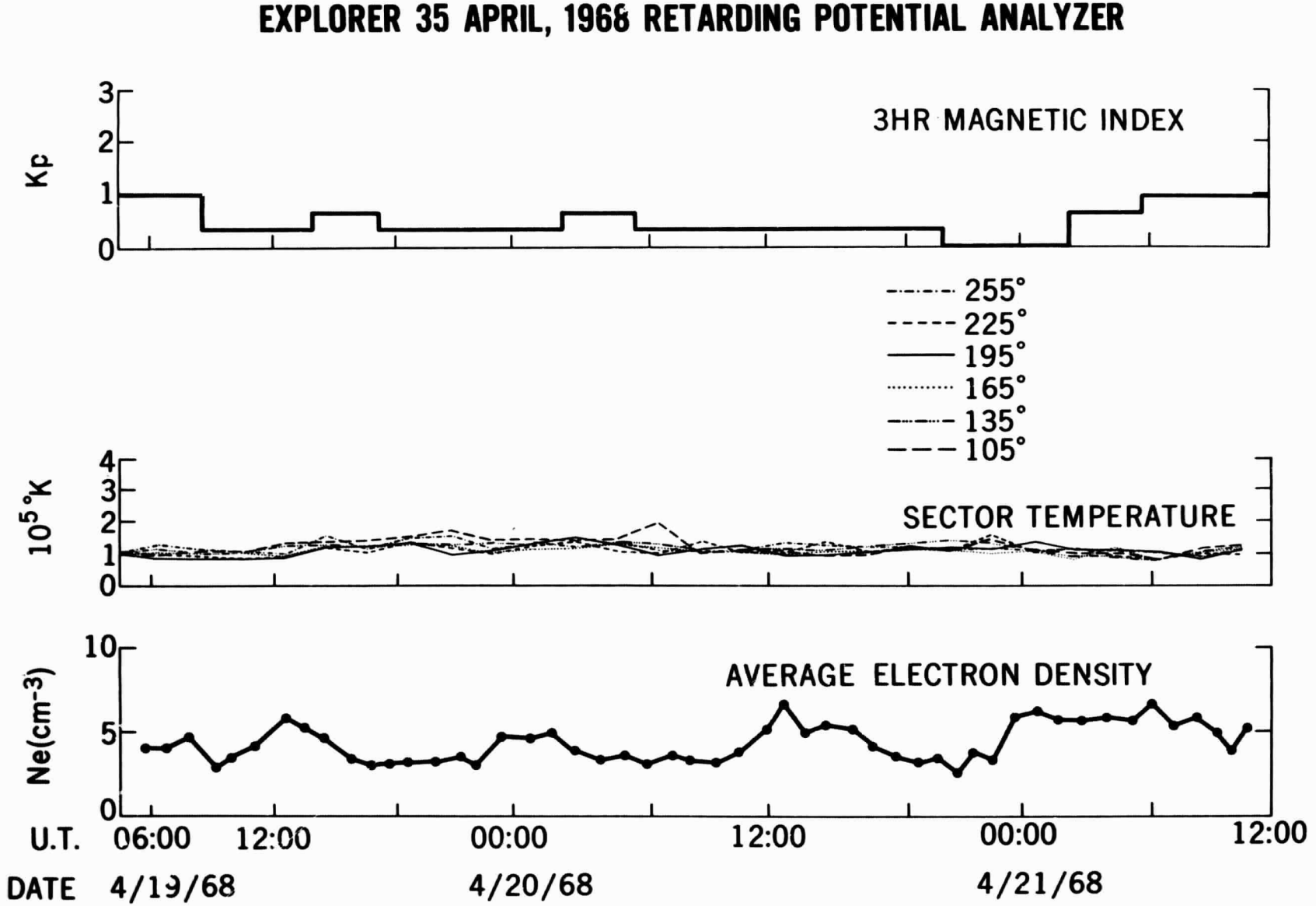
EXPLORER 35 APRIL, 1968 RETARDING POTENTIAL ANALYZER
3HR MAGNETIC INDEX
Kp
3
2
1
0
255°
225°
195°
165°
135°
105°
SECTOR TEMPERATURE
$10^5$°K
4
3
2
1
0
AVERAGE ELECTRON DENSITY
Ne(cm$^{-3}$)
10
5
0
U.T. 06:00 12:00 00:00 12:00 00:00 12:00
DATE 4/19/68 4/20/68 4/21/68

Figure 7

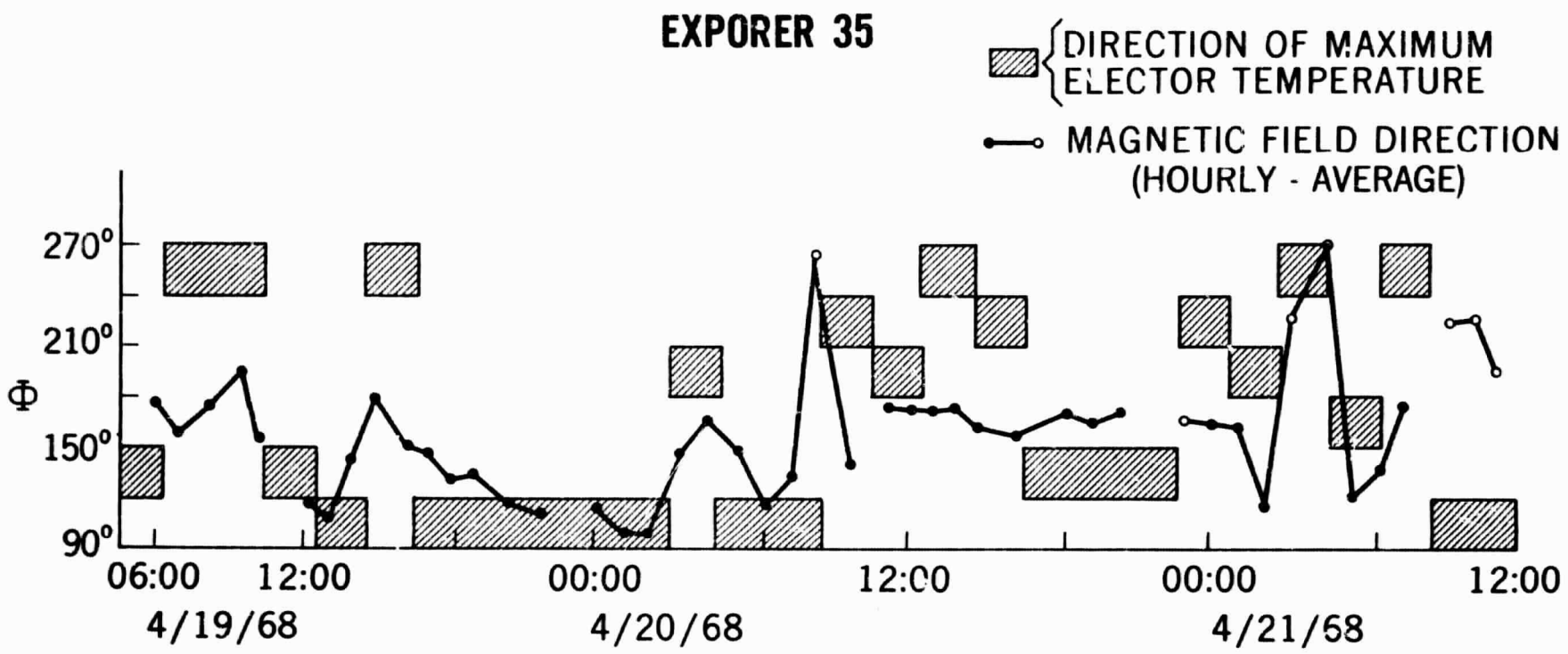
EXPORER 35
DIRECTION OF MAXIMUM ELECTOR TEMPERATURE
MAGNETIC FIELD DIRECTION (HOURLY - AVERAGE)
270°
210°
150°
90°
Φ
06:00
12:00
00:00
12:00
00:00
12:00
4/19/68
4/20/68
4/21/68

Figure 8


Kp
4
3
2
1
0
SUDDEN COMMENCEMENT 23:40 U.T.

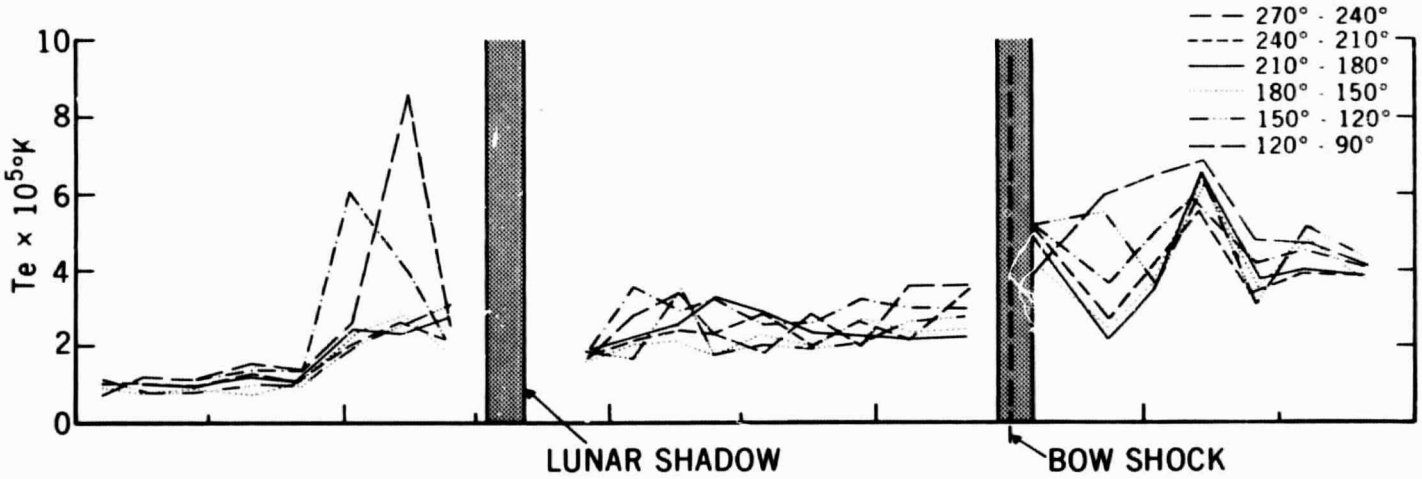
Te x 10^5°K
10
8
6
4
2
0
270° - 240°
240° - 210°
210° - 180°
180° - 150°
150° - 120°
120° - 90°
LUNAR SHADOW
BOW SHOCK

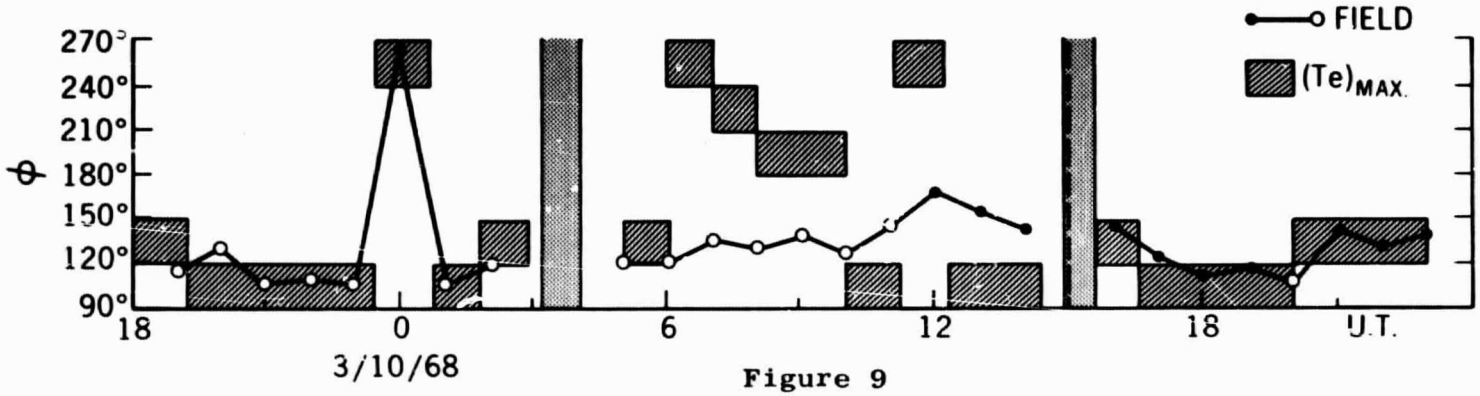
FIELD
(Te)MAX.
270°
240°
210°
180°
150°
120°
90°
ϕ
18
0
6
12
18
U.T.
3/10/68

Figure 9

# TABLE 1

| SHOCK CROSSING | TIME UT | FIELD F($\gamma$) | FIELD $\theta$ | FIELD $\Phi$ | ELECTRONS Ne | ELECTRONS $Te_{(II)}$ | ELECTRONS Ke | $1-\beta_e A_e$ |
|---|---|---|---|---|---|---|---|---|
| | 23:00 | 6.3 | - 4° | 286° | 3 | 1.44 | 1.1 | .98 |
| 23:40 UT, 9 MARCH, 1968 | 00:00 | 10 | 55° | 265° | 3 | 6.3 | 3.0 | .74 |
| MHD – SHOCK | 01:00 | 10.1 | 34° | 287° | 11 | 8.9 | 3.4 | −.17 |
| | 02:00 | 10.0 | 31° | 300° | 7 | 3.4 | 1.6 | .85 |
| | 14:00 | 10.4 | -65° | 142° | 5.0 | 3.6 | 1.5 | .90 |
| 15:00 UT, 10 MARCH, 1968 | 15:00 | – | – | – | – | – | – | ~ |
| BOW – SHOCK | 16:00 | 15.3 | 46° | 145° | 5.0 | 5.5 | 1.4 | .91 |
| | 17:00 | 14.3 | -38° | 125° | 5.0 | 5.8 | 2.7 | .74 |
| | 08:00 | 5.7 | -17° | 291° | 6 | 2.7 | 1.3 | .79 |
| 09:04 UT, 20 NOV., 1968 | 09:00 | ~ | ~ | ~ | 2.0 | 2.8 | 1.0 | ~ |
| MHD – SHOCK | 10:00 | 13.5 | 21° | 242° | 1.6 | 5.7 | 2.0 | .96 |
| | 11:00 | 13.8 | 4° | 251° | 15.6 | 2.6 | 1.4 | .92 |